

Influence of viscous effects on numerical prediction of motions of SWATH vessels in waves

Stefano Brizzolara^{*}, Luca Bonfiglio and João Seixas de Medeiros

Massachusetts Institute of Technology, MIT Sea Grant and Innovative Ship Design Lab,
77 Massachusetts Ave, 02139 Cambridge, MA, USA

(Received July 27, 2013, Revised September 20, 2013, Accepted September 25, 2013)

Abstract. The accurate prediction of motion in waves of a marine vehicle is essential to assess the maximum sea state vs. operational requirements. This is particularly true for small crafts, such as Autonomous Surface Vessels (ASV). Two different numerical methods to predict motions of a SWATH-ASV are considered: an inviscid strip theory initially developed at MIT for catamarans and then adapted for SWATHs and new a hybrid strip theory, based on the numerical solution of the radiation forces by an unsteady viscous, non-linear free surface flow solver. Motion predictions obtained by the viscous flow method are critically discussed against those obtained by potential flow strip theory. Effects of viscosity are analyzed by comparison of sectional added mass and damping calculated at different frequencies and for different sections, RAOs and motions response in irregular waves at zero speed. Some relevant conclusions can be drawn from this study: influence of viscosity is definitely non negligible for SWATH vessels like the one presented: amplitude of the pitch and heave motions predicted at the resonance frequency differ of 20% respectively and 50%; in this respect, the hybrid method with fully non-linear, viscous free surface calculation of the radiation forces turns out to be a very valuable tool to improve the accuracy of traditional strip theories, without the burden of long computational times requested by fully viscous time domain three dimensional simulations.

Keywords: seakeeping; SWATH; viscous effects; viscous added mass and damping; Navier-Stokes equations solver for oscillating floating bodies; Autonomous Surface Vessels

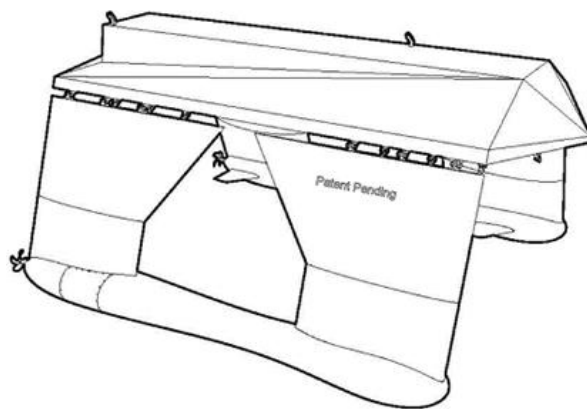
1. Introduction

A new family of Autonomous Surface Vehicles (ASVs) has been designed to achieve low motions in waves (enhance operability at sea) and reduced powering requirement at cruise speed to maximize endurance or achieve high speeds (Brizzolara and Chryssostomidis 2013). The family is based on an unconventional SWATH hull which has been optimized with respect to these two objectives resulting in a twin canted struts arrangement and a particular underwater hull shape having two maximum area sections and an intermediate minimum area section, opportunely positioned along the length to minimize the drag.

A design example of the vehicle of the family is presented in Fig. 1: it is a small (7 m long) Unmanned Surface Vehicle (USV) designed (Brizzolara *et al.* 2011) to serve a network of

^{*}Corresponding author, Professor, E-mail: stebriz@mit.edu

Autonomous Underwater Vehicles (AUVs), carrying out autonomously (or under control of a remote pilot) several types of support operations that normally would required a manned ship: these tasks include launching and recovering AUVs from the sea, underway recharging and transporting them home (to a mother ship or to a land base).



Thecnical Data		
Length Over All	[m]	7.02
Length at WL	[m]	5.9
Beam Max	[m]	5.44
Draft	[m]	1.18
Height	[m]	3.33
Displacement Full	[t]	4.343
Engine Power	[kW]	2x22
Max Speed	[knots]	12

Fig. 1 USV-SWATH for Launching, Recovering and Recharging of AUVs

These types of missions obviously require a very stable platform in waves, in terms of minimum motions in irregular sea states at almost zero speed, if not a synchronous motion behavior to the AUV that stays partially submerged during the operation of approach to be recovered or recharged. Since this last task appears to be quite impossible as a design goal and too much dependent on the particular AUV considered, the choice has been to minimize the absolute motions of the USV by adopting an unconventional hull design, such as that above introduced and presented in Fig. 1.

1.1 Prediction of the Motions in Waves of SWATHs

In the last 50 years different theoretical and numerical methods have been developed to predict motions in waves of catamarans and in particular SWATHs vessels, all in general based on the solution of the hydrodynamic problems by potential flow approximation. From general methodological approach, the methods range from strip theory approximations (Lee *et al.* 1977), to slender body theories and to three dimensional boundary element methods (Matzaris 1998, Centeno *et al.* 2010). Only recently, fully viscous flow solvers, based on the numerical solution of the Reynolds Averaged Navier Stokes Equations, have been used to solve the complete rigid body motion of a ship in waves (Carrica *et al.* 2007). Their level of accuracy goes hand in hand with the computational time needed to obtain the motion prediction in a given sea state. The Graph of Fig. 2 shows the order of magnitude of the computational time and the level of accuracy (normalized by the lowest fidelity method) of different seakeeping numerical methods. On the lower end there

are potential flow based codes, two dimensional (strip theory based) or three dimensional (panel methods) based on linear theory in frequency domain. In the case of catamarans and SWATHs (Mansour and Choo 1973) and (Lee and Curphey 1977) have been a reference for this study.

Viscosity effects can be introduced in these methods as empirical addition to damping forces (Centeno *et al.* 2000), but important uncertainties (Rathje and Schelling 1996) are introduced by this arbitrarily selected added forces, since their application is strictly valid for few simple sectional shapes and has been derived in steady state flow problems. Higher fidelity can be achieved with a non-linear time domain approach in case of large amplitude motions (Fang and Her 1995). In this case some non-linearities related to viscous corrections can be introduced, though also in these cases, they are still approximate and added through empirical motion-amplitude-dependent corrections.

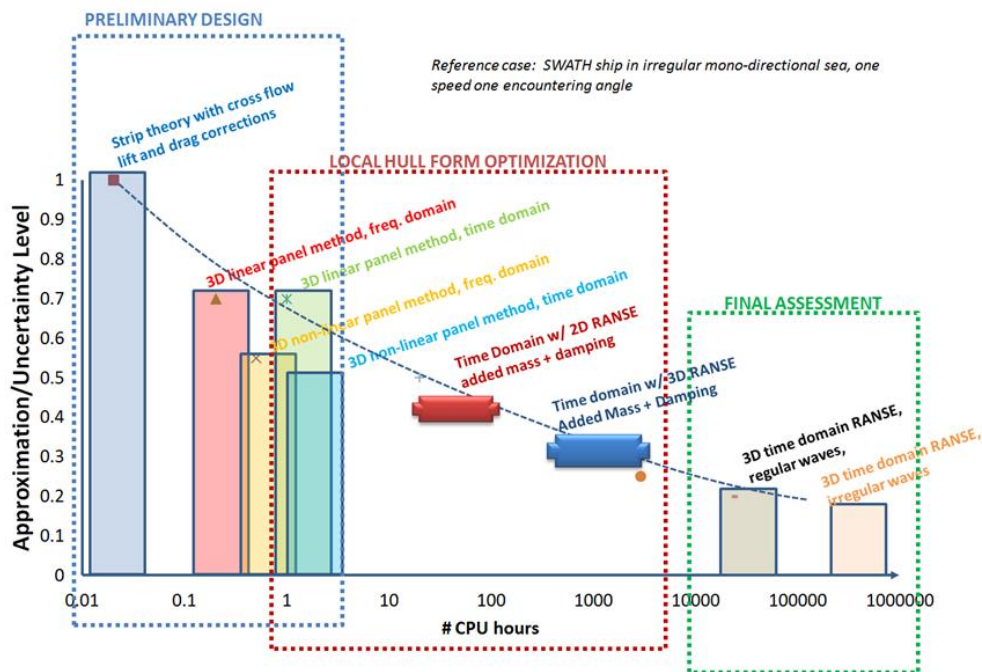


Fig. 2 Accuracy vs. computational time of different numerical methods for the motion prediction of SWATH ship in waves. Considered methods range from 2D potential flow theories to unsteady 3D viscous flow solvers

On the upper end of the time scale of the graph in Fig. 2, there are the fully viscous three dimensional, free surface transient flow solvers used to derive the Response Amplitude Operators (RAO) of motions with a series of time domain simulations in monochromatic waves or directly the time-domain motions in irregular waves (for a given sea state and encountering angle). This kind of simulations are indeed possible and their applicability has been verified offering the highest possible fidelity against model test results, but require large computational time and resources.

In between the two types of methods, potential flow based and the 3D fully viscous, there is a

gap that we are working to close. There is fact the possibility to create a hybrid frequency domain method (or time domain based on frequency domain results) by calculating the radiation forces only with viscous calculations (in 2D or 3D) and then to provide exciting and restoring forces through a classical linear potential flow approach. Wave induced forces, in fact, are minimally influenced by viscosity. On the other hand in previous numerical validation studies we demonstrated that the calculation of the damping and added mass with viscous (NS) solver can lead to excellent correlation with experimentally measured values in case of simple sections (Bonfiglio *et al.* 2012) and SWATH like sections (Bonfiglio *et al.* 2013).

Being this the goal, we start to present here a numerical study aimed to highlight the relative differences in terms of motions predicted by a classic potential flow strip theory method initially developed at MIT (Mansour and Choo 1973) and adapted to SWATHs (Chryssostomidis and Patrikalakis 1984), still widely used nowadays for basic design purposes and a new hybrid strip theory where the radiation forces are calculated by a fully viscous flow solver on 2D sections. This with the scope to eliminate the inaccuracies introduced by empirical viscous corrections to potential flow based methods that for SWATHs vessels are indeed quite important (Centeno *et al.* 2010).

2. Strip theory for swath ships

The problem of analyzing motions and loads for catamarans in a random sea state with linear theory was addressed by Mansour and Choo (1973), the proper assumptions, boundary conditions and equations were outlined. This work culminated in the development of “CAT-5D”, a strip-theory based code capable of handling such calculations for any given hull geometry, weight distribution and sea characteristics. When the method was first applied to SWATHs, Chryssostomidis and Patrikalakis (1986) passed from a fully analytical integration method over 2D sections of the original CAT-5D code, working well for typical catamarans hull forms, to a more general fully numerical integration scheme needed to avoid the singularities of sections without strut of SWATH type of vessels. A new code has been written in Matlab and it is now integrated into routine design and optimization of SWATH vehicles at MIT Innovative Ship Design lab. Hereinafter we outline the principal theoretical elements of the method.

The simplified equation of motion for a ship, considered as a rigid body, in regular waves, for the six degrees of freedom is

$$(M_{ij} + A_{ij})\ddot{\eta}_j + B_{ij}\dot{\eta}_j = F_i(t) \quad i, j = 1, 2, \dots, 6 \quad (1)$$

where M_{ij} , A_{ij} , B_{ij} and C_{ij} are 6x6 matrices representing, respectively, the ship's mass, added-mass, damping and restoring coefficients. $F(t)$ and η are 6x1 vectors representing, respectively, the forces and motions in the six degrees of freedom, $\dot{\eta}$ and $\ddot{\eta}$ are the first and second time derivatives of the motion, in other words, the velocity and acceleration of the vessel.

Eq. (1) can be simplified by considering the ship symmetric about its center plane, with usual linear assumption of decoupled motions in the horizontal and vertical planes. The simplified equations of linear seakeeping problems in the vertical plane neglecting surge motion influence

$$(M + A_{33})\ddot{\eta}_3 + B_{33}\dot{\eta}_3 + C_{33}\eta_3 + A_{35}\ddot{\eta}_5 + B_{35}\dot{\eta}_5 + C_{35}\eta_5 = F_3 e^{i\omega t} \quad (2)$$

$$A_{53}\ddot{\eta}_3 + B_{53}\dot{\eta}_3 + C_{53}\eta_3 + (I_{55} + A_{55})\ddot{\eta}_5 + B_{55}\dot{\eta}_5 + C_{55}\eta_5 = F_5 e^{i\omega t} \quad (3)$$

The strip theory assumptions permit to reduce the problem to a numerical solution of flow on 2D cross sections. Three dimensional added-mass, damping and restoring coefficients are then calculated through the integration of the two-dimensional ones over the length of the ship, see for instance Lee and Curphey (1977) where no additional viscous corrections have been used. To compute the required 2D coefficients the fluid is assumed to be inviscid, incompressible and irrotational, the environment is infinitely deep and previously undisturbed with negligible surface tension effects. The amplitude of the motions is assumed to be small. With these simplifications the problem reduces to the calculation of a (complex) velocity potential in the form

$$\phi^m(y, z, t) = \text{Re} \left\{ \phi^m(y, z) e^{-i\omega t} \right\} \tag{4}$$

$$\phi^m = \phi_c^m + i \phi_s^m \tag{5}$$

where $m = 2$ (sway), 3 (heave), 4 (roll) are the three degree of freedom of the transverse plane reduced motion problem.

The perturbation velocity potential flow problem is defined by the following conditions

$$\text{Laplace Equation} \quad \nabla^2 \phi^m = 0 \quad \text{for } z < 0 \tag{6}$$

$$\text{Linearized Free-Surface Condition} \quad \frac{\partial^2 \phi^m}{\partial t^2} + g \frac{\partial \phi^m}{\partial z} = 0 \quad \text{for } z = 0 \tag{7}$$

$$\text{The Deep Water Boundary Condition} \quad \lim_{z \rightarrow -\infty} |\nabla \phi^m| = 0 \tag{8}$$

$$\text{The Radiation Condition} \quad \lim_{y \rightarrow \pm\infty} \left(\frac{\partial \phi^m}{\partial y} \pm i K \phi^m \right) = 0 \quad \text{where } K = \frac{\omega^2}{g} \tag{9}$$

$$\text{The Symmetry Condition} \quad \frac{\partial \phi^3}{\partial y}(0, z, t) = 0 \quad \text{and} \quad \phi^2(0, z, t) = \phi^4(0, z, t) = 0 \tag{10}$$

$$\text{Linearized Hull Boundary Condition} \quad \vec{n} \cdot \nabla \phi^m = v_n^m \tag{11}$$

where \vec{n} is the outward unit normal vector on the hull and v_n^m is the normal component of the normal velocity of the hull due to forced oscillations.

Through Frank source method (1967) based on Green's functions, the velocity potential can be calculated distributing two dimensional pulsating sources along the hull contour with strength given by

$$G_R^m(w, \zeta, t) = \text{Re} \left\{ G_R^m(w, \zeta) e^{-i\omega t} \right\} \tag{12}$$

where $G_R^m(w, \zeta) = G_{RC}^m(y, z; \xi, \eta) + i G_{RS}^m(y, z; \xi, \eta)$ (13)

$$G_{RC}^m = \frac{1}{2\pi} \text{Re} \left\{ \left[\text{In} \frac{(w - \zeta)}{(w - \bar{\zeta})} + 2 \int_0^\infty \frac{e^{-ik(w - \bar{\zeta})}}{K - k} dk \right] - (-1)^m \left[\text{In} \frac{(w + \bar{\zeta})}{(w + \zeta)} + 2 \int_0^\infty \frac{e^{-ik(w - \bar{\zeta})}}{K - k} dk \right] \right\} \tag{14}$$

$$G_{RS}^m = -\text{Re} \left\{ e^{-ik(w - \zeta)} - (-1)^m e^{ik(w + \zeta)} \right\} \tag{15}$$

$w = y + i z$ is the field point, $\zeta = \xi + i \eta$ is the source point

The time-independent part of the velocity potential can be calculated through a contour integral of the source singularities of unknown strength along the hull.

$$\phi^m(y, z) = \oint_{C_x} Q(s) G_R^m(y, z; s) ds \quad (16)$$

where C_x is the immersed contour at the desired section x .

$$Q(s) = Q_c + i Q_s = \text{Source Density} \quad (17)$$

the source density is determined by imposing the Kinematic Boundary Condition.

$$(\vec{n} \cdot \nabla) \left[\oint_{C_x} Q_C(s) G_{RC}^m(y, z; s) ds - \oint_{C_x} Q_S(s) G_{RS}^m(y, z; s) ds \right] = A \omega n_i^m \quad (18)$$

$$(\vec{n} \cdot \nabla) \left[\oint_{C_x} Q_C(s) G_{RS}^m(y, z; s) ds - \oint_{C_x} Q_S(s) G_{RC}^m(y, z; s) ds \right] = 0 \quad (19)$$

These integrals can be numerically solved when the hull is subdivided in N straight line segments and the sources of unknown strength distributed over each segment. Then above integral Eqs. (18) and (19) become

$$\sum_{j=1}^N Q_{Cj} I_{ij}^m - \sum_{j=1}^N Q_{Sj} J_{ij}^m = A \omega n_i^m \quad (20)$$

$$\sum_{j=1}^N Q_{Cj} J_{ij}^m + \sum_{j=1}^N Q_{Sj} I_{ij}^m = 0 \quad (21)$$

Where

$$Q_j = Q_{Cj} + \bar{J} Q_{Sj} \quad \bar{J} = \sqrt{-1} \quad (22)$$

$$I_{ij}^m = \left[(\vec{n} \cdot \nabla) \oint_{C_j} G_{RC}^m ds \right] \quad (y = y_i \text{ and } z = z_i) \quad (23)$$

$$J_{ij}^m = \left[(\vec{n} \cdot \nabla) \oint_{C_j} G_{RS}^m ds \right] \quad (y = y_i \text{ and } z = z_t) \quad (24)$$

$$\vec{n} \text{ at } C_i = (\sin(a_i) - \cos(a_i)) \quad a_i = t a \vec{n} \frac{(\eta_{i+1} - \eta_i)}{(\xi_{i+1} - \xi_i)} \quad (25)$$

The potential is then numerically approximated through the equation

$$\phi^m(y_i, z_i) = \sum_{j=1}^N (Q_{Cj} I_j^m - Q_{Sj} J_j^m) + i \cdot \sum_{j=1}^N (Q_{Cj} J_j^m + Q_{Sj} I_j^m) \quad (26)$$

where

$$I_j^m = \left[\oint_{C_j} G_{RC}^m(y_i, z_i; s) ds \right] \quad J_j^m = \left[\oint_{C_j} G_{RS}^m(y_i, z_i; s) ds \right] \quad (27)$$

The total force or moment, F^m , is obtained by integrating the pressure given by the linearized Bernoulli equation. The 2D added-mass and damping can be obtained from

$$F^m = -a_{mm} \ddot{I}(t) - b_{mm} \dot{I}(t) =$$

$$\left[-2\rho\omega \oint_{C_x} \phi_C(y_i, z_i) \cdot \vec{n} ds \right] \sin(\omega t) + \left[2\rho\omega \oint_{C_x} \phi_S(y_i, z_i) \cdot \vec{n} ds \right] \cos(\omega t) \quad (28)$$

which leads to
$$a_{mm} = -\frac{2\rho}{A\omega} \oint_{C_x} \phi_C \cdot \vec{n} ds \quad b_{mm} = -\frac{2\rho}{A} \oint_{C_x} \phi_S \cdot \vec{n} ds \quad (29)$$

The kernel and potential integrals $I_{ij}^m, J_{ij}^m, I_j^m$ and J_j^m are evaluated in a similar manner as given in Frank (1967).

The three dimensional coefficients, for the zero speed problem considered in this study, are calculated by integration along the hull length as from Table 1.

Table 1 3D added mass and damping definition formulae

$A_{33} = \int a_{33} dx$	$B_{33} = \int b_{33} dx$
$A_{35} = A_{53} = -\int x a_{33} dx$	$B_{35} = B_{53} = -\int x b_{33} dx$
$A_{55} = \int x^2 a_{33} dx$	$B_{55} = \int x^2 b_{33} dx$

According standard linear theory the responses are calculated solving the system (2) of two equations in two unknowns (η_3 and η_5) when correctly projected in frequency domain (Lee and Curphey 1977).

3. Viscous solution of the radiation problem

We supply here the basic details of the Navier-Stokes solver used for the calculation of the viscous added mass and damping of the 2D sections. The method has been first applied and successfully validated for simple singular sections (Bonfiglio *et al.* 2012) then for twin sections and recently also for SWATH like sections (Bonfiglio *et al.* 2013) with very good correlation with experimental results.

The conservation law for mass and momentum applied to a Newtonian incompressible fluid leads to the Navier-Stokes equations, that written in a Cartesian reference frame in a non-conservative form

$$\frac{\partial(\rho u_i)}{\partial(x_i)} \quad (29)$$

$$\frac{\partial u_i}{\partial t} + \frac{\partial(u_i u_j)}{\partial x_i} = \frac{\partial}{\partial x_i} \left(\nu \frac{\partial u_i}{\partial x_i} \right) - \frac{1}{\rho} \frac{\partial u_i}{\partial x_i} + g_i \quad (30)$$

The system is a set of partial differential non linear equations in the unknowns of pressure and velocity components.

A fully non-linear viscous method is proposed to predict the velocity and pressure field through the numerical solution of the Navier-Stokes equations, performed exploiting a finite volume

technique in which a collocated arrangement is used to store the values of the unknown dependent variables: pressure and velocities are evaluated for the same control volume at the centroids of each cell.

The structure of the momentum Eq. (30) suggests to determine the velocity components of the flow. Instead, using the continuity Eq. (29) that contains only the velocity terms, the pressure is found by the solution of a Poisson equation obtained from the divergence of the momentum equation for an incompressible fluid

$$\frac{\partial}{\partial x_i} \left(\frac{\partial p}{\partial x_i} \right) = - \frac{\partial}{\partial x_i} \left[\frac{\partial (\rho u_i u_j)}{\partial x_j} \right] \quad (31)$$

The numerical solution of this equation together with the solution of the velocity equation (momentum equation) is performed in OpenFOAM through the PISO scheme (Pressure Implicit with Splitting of Operators) introduced by Issa (1985).

Since the integrands which compare in the conservation equation are not known over all CV or over all CV faces, approximations and interpolations are required in order to evaluate values in other point of CV faces. The time derivative is numerically solved with a Euler implicit scheme, while the interpolations to determine face values, are performed through the central differential scheme. Spatial derivatives, required for the gradients that appear in the velocity and pressure equations, are evaluated using a linear central differential scheme. The same scheme is used for the interpolation of the viscosity ν in the diffusive term $\nabla(\nu \nabla U)$, where ∇U is interpolated through an explicit scheme with non-orthogonal correction (generally used for all surface normal gradients). Convection terms, that depend also on the scalar volume fraction of water in each cell (a scalar representing the quantity of water in each cell), are interpolated using a vanLeer scheme, which is specifically designed for bounded flow fields.

The sharp free surface between air and water is well captured by the volume of fluid approach that permits to solve the Navier-Stokes equations with respect to a single fluid mixture whose density and viscosity depend on the local concentration the two phases. The concentration is defined by an additional scalar, the volume fraction or indicator function α , which is normalized from 0 to 1 all over the domain.

The indicator function can be considered as a time dependent scalar field that is found through the solution of the following conservation and transport equations

$$\frac{d\alpha}{dt} = 0 \quad \Rightarrow \quad \frac{\partial \alpha}{\partial t} + \nabla \cdot \alpha U = 0 \quad (32)$$

Particular attention in the discretization and solution of the transport equation is required to fulfill the boundness criteria of α and to preserve the sharpness of the interface. For this purpose, in the present study, the method proposed by Berberovic *et al.* (2009) is used, that consists in the addition of a correction sharpening term in the transport equation

$$\frac{\partial \alpha}{\partial t} + \nabla \cdot \alpha U + \nabla \cdot [U_R \alpha (1 - \alpha)] = 0 \quad (33)$$

where a U_R is the relative velocity between air and water and the compression term $\nabla [U_R \alpha (1 - \alpha)]$ is introduced in order to preserve the sharpness of the free surface.

A series of unsteady free surface viscous simulations models already tested and validated on simple section shapes (Bonfiglio *et al.* 2012) also in catamaran configurations (Bonfiglio and Brizzolara 2013). More details about the numerical model can be found in the cited papers.

Once the time history of the radiation force component (in the selected direction) is obtained from each simulation, at each given oscillation frequency (and degree of freedom: heave in this case), the results are projected from time domain to frequency domain applying the Fourier analysis which is used to calculate the real and the imaginary part of the force for the k^{th} harmonic

$$\begin{aligned} \text{Re } F_{33}(k\omega_k) &= \int_{t_0}^{t_1} F_{33}(t) \cos(2\pi k \bar{\omega} t) dt \\ \text{Im } F_{33}(k\omega_k) &= \int_{t_0}^{t_1} F_{33}(t) \sin(2\pi k \bar{\omega} t) dt \end{aligned} \quad (34)$$

in which $\bar{\omega}$ represents the forced oscillation frequency.

According linear seakeeping theory the added mass and damping coefficient are obtained from the 1st harmonic obtained by the Fourier analysis, i.e., the force component characterized by the same frequency of the motion. Considering the sinusoidal motion amplitude of ξ_k imposed in the transient simulation, sectional added mass and damping coefficient are expressed as follow

$$a_{33}(\omega_k) = -\frac{\text{Re } F_{33}(\omega_k)}{\omega_k^2 \xi_3} \quad b_{33}(\omega_k) = \frac{\text{Im } F_{33}(\omega_k)}{\omega_k \xi_3} \quad (35)$$

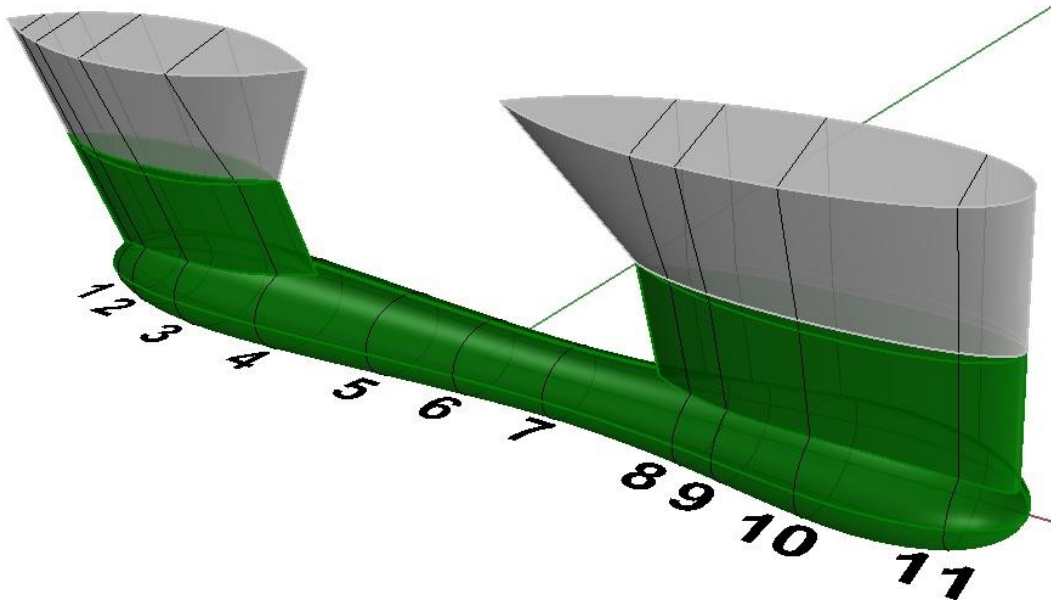


Fig. 3 Geometry of a SWATH demi-hull with position of the 11 sections (from stern to bow) considered to calculate the viscous added mass and damping (reference system origin is at LCG)

4. Results

Following the strip theory approach, the 3D geometry of the SWATH has been represented with 11 sections along the length that are presented and numbered in Fig. 3. The sections have been selected considering a non-uniform spacing to minimize their number without compromising accuracy (sensitivity analysis tests were done).

As anticipated, radiation forces have been estimated at each section with the two different approaches: potential flow (Frank's close fit method with 50 points along the section) and the viscous method based on the solution of the transient N-S equation for the oscillating sections in calm water. The numerical simulations have been performed for a model in scale 1:6 to the actual vessel (i.e., submerged hull length $L=1\text{m}$). The amplitude of the vertical oscillatory motion for the viscous calculations has been set to $2.5\% \cdot L \equiv 0.0127 \cdot T$, where $T=\text{draft}$.

Only vertical plane motions are discussed in this paper, i.e., only heave and pitch motions related coefficients. This means that only the problem of the 11 vertical oscillating sections has been considered and solved with the viscous free surface N-S solver. For SWATH vessels in general and in particular for the twin canted struts version considered in this study, viscous effects are important not only for the transverse motions but also for heave and pitch. In fact, for these last motions, wave damping is relatively low or comparable to the viscous forces when far from the resonant frequencies (piston effect).

The nature of viscous effects can be evinced from the snapshots of Fig. 4 that presents the vorticity field for three stations along the hull length having different typologies: a thin strut (st.1), a larger strut (st.4) and a fully submerged section (st.6). Vorticity generated by separation of the flow along the struts due to the vertical oscillating motion or in the alternate wake of the elliptic section are noted and principally contribute to the viscous damping and added mass which is neglected by the presented potential flow based method. In case of the first two sections a frequency close to the resonance of the piston effect has been chosen to highlight the complex interaction between vorticity and free surface: vortexes shed by the struts are convected to the free surface and interact with wave induced flow field, enhancing or reducing their intensities. Especially in the case of section 4, a strong non-linear effect on the generated wave created by the strut portion above the design waterline is noted: this effect is again neglected by traditional linearized seakeeping methods. Obviously the relative importance of these non-linear effects (both generation of the inner wave and vortex shedding) is somehow enhanced by the two dimensional approach adopted. Future studies on how the three-dimensionality of the flow can affect these are under development.

The importance of viscosity is quite evident when the sectional added mass and damping calculated by the two different methods are compared. To this scope the series of graphs of Fig. 5 have been prepared. They present the calculated values of added mass and damping coefficients along the length of the vessel for three different frequencies, among those considered in the study: low, medium and high.

As expected, the added mass of sections without strut is not influenced by viscous effects: the predicted value of a_{33} for the three midship sections is the same for the two methods. Instead, for the sections with struts (four at bow and four at stern), a_{33} increases at relatively low circular frequencies (wave lengths $\lambda \geq 3L$), while it decreases at relatively high circular frequencies ($\lambda \leq 2L$).

The damping coefficients calculated with the viscous flow solver show the same trend of the inviscid ones, but they are generally higher both for sections without strut, as generally expected,

and also for the sections with struts. This is not always the case when the strut is vertical, while the present canted strut design does create additional damping. Around the resonant frequency of the piston mode effect ($\omega = 5.03$), the non-linear effects related to the amplified standing wave in between the two hulls, drastically increase the damping force on the strut sections by about a factor 4 with respect to subcritical or supercritical frequencies: this is evident comparing the end scale of the three graphs for damping.

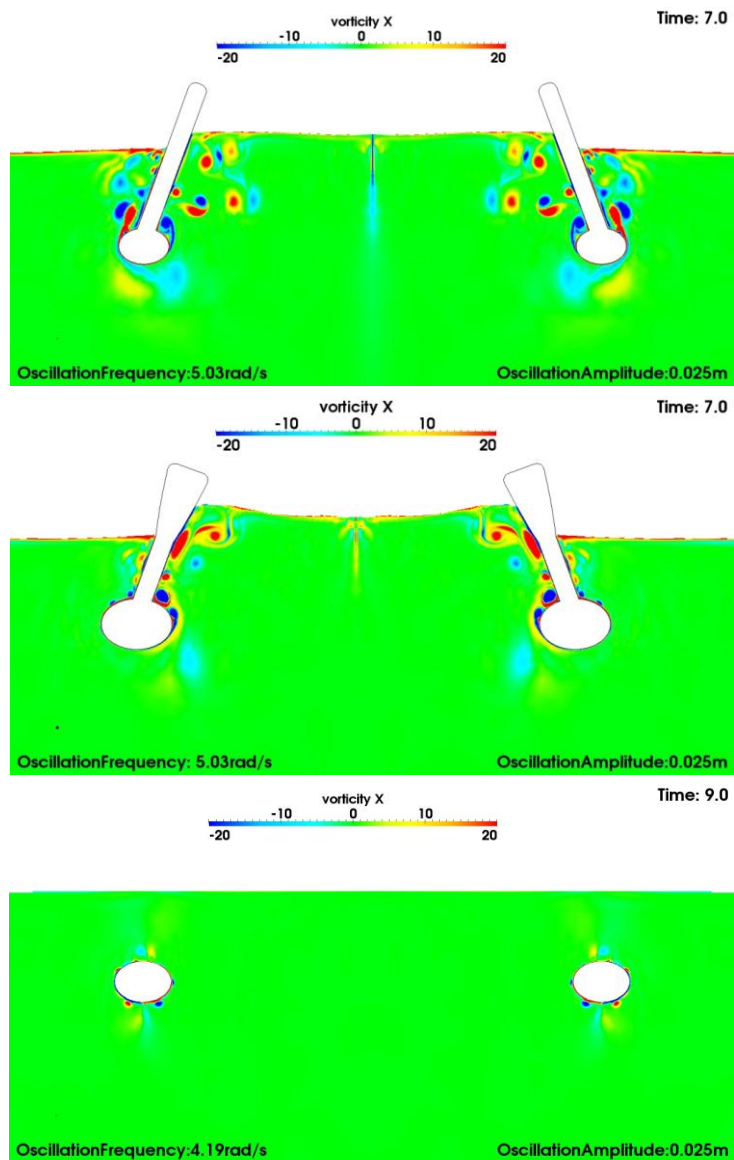


Fig. 4 Snapshot of the predicted viscous flow field (vorticity) for station 1, 4 and 6 respectively for the heave radiation problem

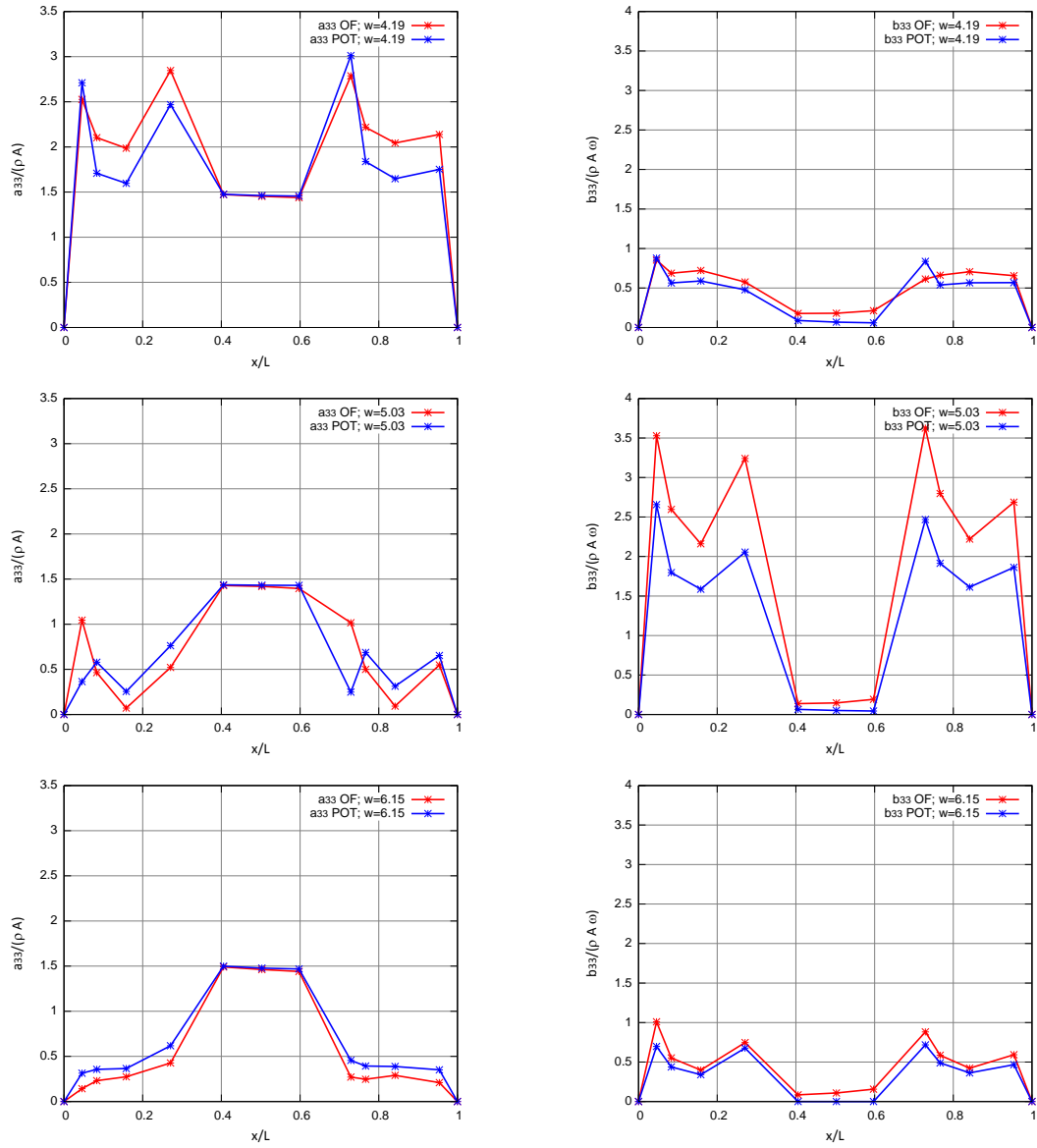


Fig. 5 Sectional heave added mass (a_{33}) and damping (b_{33}) calculated with inviscid (POT) and viscous (OF) methods at three different oscillation frequencies plot along ship length

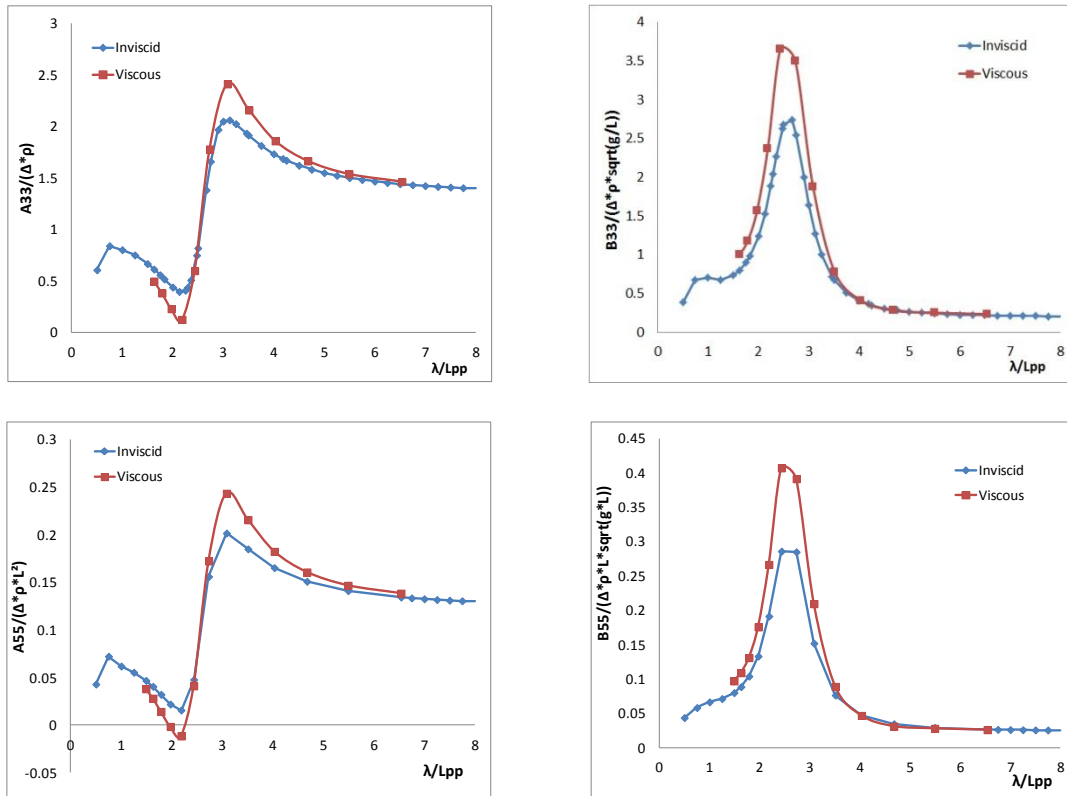


Fig. 6 Three dimensional (global) added mass and damping for heave (A_{33} , B_{33}) and pitch (A_{55} , B_{55}) calculated with Frank close fit and with Viscous (N-S) flow solver

When integrated along the length, according to formulae in Table 1, the effects just commented for the individual transverse sections become even more evident, as captured in Fig. 6 : the heave added mass of the whole hull increases at lower frequencies ($\lambda \geq 3L$) and decreases at higher frequencies ($\lambda \leq 2L$); the relative difference at the peaks amounts to more than 20%.

Simultaneously, the damping is generally increased with relative a difference of about 35÷50% around the peak.

The relevance of viscous and non-linear free surface effects in terms of motion response is given in Fig. 6, where the R.A.O. of heave and pitch are presented. At higher frequencies (low λ/L values), the predicted vertical motions amplitudes show the correct monotonic trend to zero.

Two different peaks are evident in the heave and pitch RAOs: the first, at $\lambda \approx 2.7L$, is due to the resonance frequency of the wave generated inside the two hulls (piston mode effect) which in turn depends on the separation and shape of the two hulls and in fact corresponds with the peak of the damping in Fig. 6 , while the second peak noted at higher wave lengths is due to the effect of the wave exciting forces.

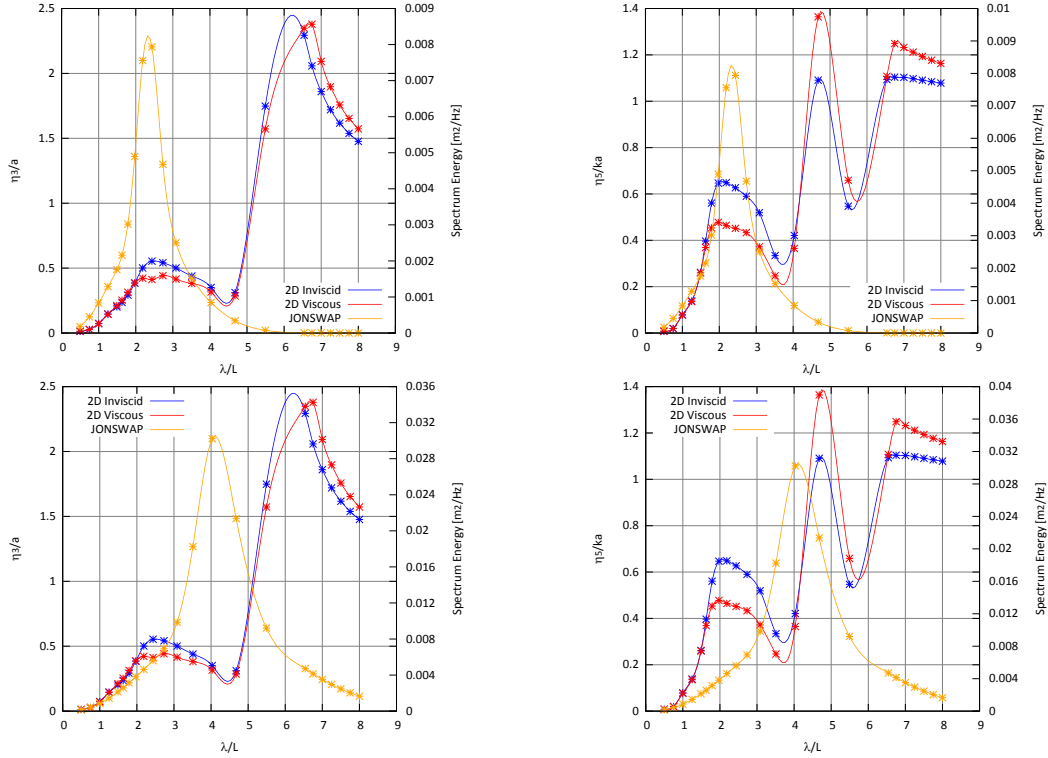


Fig. 7 Response Amplitude Operators of Heave (η_3) and Pitch (η_5) calculated by the two methods with JONSWAP

Around the first peak frequency, the heave motion amplitude predicted with the viscous method are about 15% lower than that predicted by the inviscid strip theory. The difference is even more relevant for the pitch angle: around the inner wave resonance frequency ($\lambda \approx 2.7L$) the value predicted by the viscous method is about one half (0.5!) of that predicted by the inviscid theory.

To predict the response of the vessel in a more realistic sea condition, spectral wave theory has been used with linear frequency domain seakeeping theory. Being the intended operation of for the considered autonomous vehicle concentrated in coastal areas, JONSWAP (JOINT North Sea Wave Project) spectra have been chosen to characterize the most probable irregular sea state. For practical purpose we repeat here the mathematical description of JONSWAP spectra which defines a relation between the distribution of the energy and the frequency of each elementary component

$$S(\omega) = \frac{ag^2}{\omega^5} e - \beta \frac{\omega_p^4}{\omega^4} \gamma^a \quad (36)$$

Spectral peak sharpness is modeled through the peak enhancement parameter γ which ranges from 1 to 7 with the mean value of 3.3, that is the one chosen in the present analysis.

$$a = \exp \left[-\frac{(\omega - \omega_p)^2}{2\omega_p^2\sigma^2} \right] \quad \text{and} \quad \sigma = \begin{cases} 0.07 & \text{if } \omega \leq \omega_p \\ 0.09 & \text{if } \omega \geq \omega_p \end{cases} \quad (37)$$

The shape of the distribution is mainly tuned by the parameter β , for which we selected a typical value is 1.25. The parameter α represents the intensity of the spectra and can be related to the wind speed, according the following empirical formula

$$\alpha = 5.061 * \left(\frac{\omega}{p}\right)^4 * (H_s^2) * (1 - 0.287 * \ln(\gamma)) \quad (38)$$

Fig. 7 shows the SWATH RAO with the irregular head sea energy spectra superimposed. This allows to better visual evaluation of the matching between the relative position of the peak of the wave spectrum relative to the RAO peak. Significant wave height and peak frequency chosen to define the wave spectra correspond to the most probable sea state conditions in the area of operation of the SWATH.

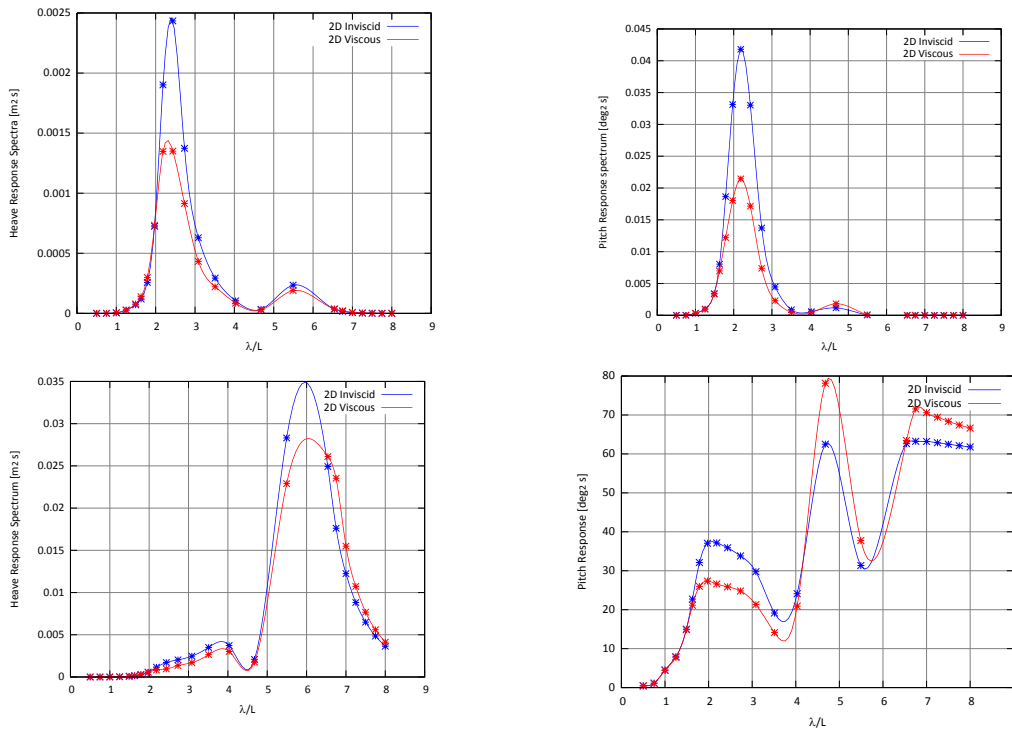


Fig. 8 Response spectra for Heave (η_3) and Pitch (η_5) amplitude for $h_{1/3}=0.3$ (top) and $h_{1/3}=0.5$ (bottom) irregular waves (see Table 2)

According linear seakeeping theory, the response spectrum of the vessel motion at zero speed has been calculated by

$$S_{\eta}(\omega) = |R.A.O. |_{\eta}^2 * S(\omega) \quad (39)$$

Assuming a narrow banded response spectrum, the significant value of the response amplitude is estimated from the zero order moment of the response spectra

$$\text{Significant Response Amplitude} = \eta_{i/3} = 2 \sqrt{\int_{-\infty}^{\infty} S_{\eta}(\omega) d\omega} \quad (40)$$

The significant value of the heave and pitch amplitudes predicted by the two different methods for each considered sea state is reported in Table 2. The difference in the predicted response depends on the characteristics of the irregular sea condition and the motion RAO: the first spectrum has a shorter peak period and most of the energy of the irregular wave is concentrated in a wave length range ($\lambda \approx 2.3L$) where viscous effects significantly reduce the amplitude of the motions (with respect to potential flow predictions). The second irregular wave spectrum, instead, has the energy content shifted to higher wave lengths ($\lambda \approx 4L$). At wave lengths higher than the sea spectrum peak, the viscous RAO is higher than that predicted by the inviscid theory and hence the viscous response becomes also higher (3rd and 4th plots of Fig. 8). The reason of this overestimation of pitch and heave by the viscous method can be found in the different values of added mass and damping predicted by the two methods in the higher wave lengths range. In fact, as from Fig. 6, for $\lambda > 4L$ the viscous and inviscid damping are practically coincident while the viscous added mass is still higher; this difference in radiation forces translate into a higher response predicted by viscous method. This is true both for heave and pitch.

Table 2 Significant pitch and heave amplitudes calculated by the two methods (potential flow based POT and viscous OF) in two different irregular head waves

SPECTRUM	$h_{1/3}$	ω_P	$\eta_{heave\ 1/3\ POT}$	$\eta_{pitch\ 1/3\ POT}$	$\eta_{heave\ 1/3\ OF}$	$\eta_{pitch\ 1/3\ OF}$
[/]	[m]	[rad/s]	[m]	[deg]	[m]	[deg]
JONSWAP1	0.3	2.0944	0.062	2.08	0.052	1.60
JONSWAP2	0.5	1.5708	0.179	2.67	0.170	2.53

5. Conclusions

A hybrid strip theory method for calculating motions of SWATHs vessels in waves based on fully numerical predictions of viscous radiation forces has been outlined in its principal theoretical and numerical aspects. The method is based on a traditional strip theory developed at MIT for catamarans and SWATHs where the radiation problem is solved by an unsteady viscous fully non-linear free surface Navier-Stokes solver, built on OpenFoam libraries. Added mass and damping of the hull cross sections are obtained from the time history of the calculated viscous force acting on the oscillating sections by Fourier analysis and used inside the strip theory instead of the inviscid ones. The difference between the hydrodynamic radiation forces predicted by the viscous and the inviscid (Frank's close fit) methods are very significant and commented in the paper.

The physical nature and relative importance of viscous effects is critically discussed through the analysis of the predicted viscous flow vorticity field around the different types of sections of the hull.

As a general results, viscosity effects are markedly non-negligible for the prediction of the motions in of the unconventional SWATH considered in this study: the difference in the predicted amplitudes of heave ad pitch motions around the characteristic piston mode resonance frequency of the SWATH is about -20% and -50% respectively (viscous against inviscid).

Two different JONSWAP wave spectra has been used to predict SWATH behavior in irregular waves, these spectra are supposed to describe with the realistic sea state conditions that a coastal operating craft has to deal with. The response amplitude values show that neglecting viscous effect leads to an overestimation of vertical motion amplitudes that reaches 50% around the resonance peak, confirming the importance of properly considering improvement achievable even in a framework of a two dimensional analysis.

No empirical correction formulae exists or can be developed to accurately predict the effect of these complex non-linear phenomena above briefly described for a general SWATH geometry. From this point of view, the current hybrid (viscous/inviscid) strip theory method offers a unique opportunity to enhance the fidelity of the predicted motions in waves, without the burden of long computational times needed by fully 3D time domain viscous free surface solvers.

Future studies will continue the application, verification and validation of the viscous strip theory method with viscous time domain 3D solvers and with experiments on a model of the AUV-SWATH presented in this study, currently under construction at the MIT Innovative Ship (I-Ship) design lab.

Aknowledgements

The research has been partially funded by the Office of Naval Research through ONR grants N00014-11-1-0598 and N00014-13-1-0398 with C. Chryssostomidis and S. Brizzolara as primary investigators. The authors are thankful to Dr. Kelly Cooper and Sharon Beermann Curtin for supporting these research projects.

References

- Bonfiglio, L. Brizzolara, S. and Chryssostomidis, C. (2012), "Added mass and damping of oscillating bodies: a fully viscous numerical approach", *Proceedings of the 9th WSEAS International Conference on Fluid Mechanics (FLUIDS '12)*, Harvard, Cambridge, USA, 25-27 January.
- Bonfiglio, L. Brizzolara, S. and Chryssostomidis, C. (2013), "Viscous free surface numerical simulations of oscillating SWATH ship sections", *Proceedings of the 10th WSEAS International Conference on Fluid Mechanics. FLUIDS'13*, Milano, Italy, 9-11 January.
- Bonfiglio, L. and Brizzolara, S. (2013), "Influence of viscosity on radiation forces: a comparison between monohull", *Proceedings of the Catamaran and SWATH. ISOPE 2013, the 23rd International Ocean and Polar Engineering Conference*, Anchorage, Alaska, USA, 1-5 July.
- Brizzolara, S., Curtin, T., Bovio, M. and Vernengo, G. (2011), "Concept design and hydrodynamic optimization of an innovative SWATH USV by CFD methods", *Ocean Dynam.*, **61**, ISSN: 1616-7341, doi: 10.1007/s10236-011-0471-y.
- Brizzolara, S. and Chryssostomidis, C. (2013), "The second generation of unmanned surface vehicles:

- design features and performance predictions by numerical simulations”, *Proceedings of the ASNE Day 2013*, Engineering America's Maritime Dominance, Arlington, VA, 21-22 February.
- Brizzolara, S. and Vernengo, G. (2011), “Automatic optimization computational method for unconventional S.W.A.T.H. ships resistance”, *Int. J. Math. Model. Method. Appl. Sci.*, **5**, 882-889.
- Carrica, P.M., Wilson, R.V., Noack, R. and Stern, F. (2007), “Ship motions using single-phase level set with dynamic overset grids”, *Comput. Fluids*, **36**, 1415-1433.
- Centeno, R., Fonseca, N. and Guedes Soares, C. (2010), “Prediction of motions of catamarans accounting for viscous effects”, *Int. Shipbuild. Progr.*, **47**(451), 303-323.
- Chrysostomidis, C. and Patrikalakis, N.M. (1986), *Seakeeping calculations for SWATH ships using a new modified version of 'CAT-5'*, MIT Sea Grant Report 86-7TN.
- Fang, M.C. and Her, S.S. (1995), “Non-linear SWATH ship motions in large longitudinal waves”, *Int. Shipbuild. Progr.*, **42**(431), 197-220.
- Frank, W. (1967), *Oscillation of cylinders in or below the free surface of deep fluids*, NSRDC Report No. 2375.
- Lee, C.M. and Curphey, R.M. (1977), “Prediction of motion stability and wave load of small-waterplane-area, Twin-Hull Ships”, *SNAME Trans.*, **85**, 94-130.
- Mansour, A. and Choo, K.Y. (1973), *Motion and loads prediction of catamarans in random seas*, Report 73-6, MIT, Dept. of Ocean Engineering.
- Mantzaris, D.A. (1998), *A rankine panel method as a tool for the hydrodynamic design of complex marine vehicles*, PhD Thesis, MIT Ocean Engineering Dept.
- Rathje, H. and Schelling, T.E. (1996), “Dependence of SWATH ship response in waves on choice of viscous coefficients”, *Proceedings of the 11th Int. Workshop On Water Waves And Floating Bodies*, Institut fur Schiffbau, Hamburg.